moments are one-dimensional they are of finite length. Therefore, each chain consists of domains of parallel moments; the direction of the moments at each domain is antiparallel to the direction of the moments in its adjacent domains. The domain boundary point moves along the chain giving rise to the relaxation phenomenon. In the intermediate temperature range, as the temperature decreases the intrachain correlation length (size of the domain) increases until at $T = T_N =$ 9·5 K three-dimensional long-range order sets in. At this point the correlations along the ZC's increase to infinity and a long-range order between the ZC's sets in. At temperatures slightly above T_N the ferromagnetic correlation within each chain, ferromagnetic domain, are of some finite length. Therefore, when the coupling between the chains sets in, it induces an emergence of a large contribution to the magnetic scattering at the Bragg angle as exhibited by the abrupt change in the magnetization curve (Fig. 3) at T_N.

References

AMIT, M., HOROWITZ, A. & MAKOVSKY, J. (1974). *Isr. J. Chem.* **12**, 827–830.

GUREWITZ, E., HOROWITZ, A. & SHAKED, H. (1979). *Phys. Rev. B*, **20**, 4544–4549.

GUREWITZ, E., MAKOVSKY, J. & ATZMONY, U. (1976). *Phys. Rev. B*, **13**, 375–378.

GUREWITZ, E., MAKOVSKY, J. & SHAKED, H. (1974). *Phys. Rev. B*, 9, 1071–1076.

GUREWITZ, E. & SHAKED, H. (1972). *Acta Cryst.* A**28**, 280–284.

WATSON, R. E. & FREEMAN, A. J. (1961). *Acta Cryst.* **14**, 27–37.

WYCKOFF, R. W. G. (1964). *Crystal Structures*, Vol. 2, 2nd ed., p. 430. New York: John Wiley.

Acta Cryst. (1982). B**38**, 2775–2781

The Preparation and Structure of Barium Uranium Oxide $BaUO_{3+x}$

BY S. A. BARRETT

*Inorganic Chemistry Laboratory, South Parks Road, Oxford OX*1 3*QR, England*

A. J. JACOBSON

Exxon Research and Engineering Co., PO Box 45 *Linden, New Jersey* 07036, *USA*

B. C. TOFIELD

*AERE, Harwell, Didcot, Oxfordshire OX*11 0*RA, England*

AND B. E. F. FENDER

Institut Laue–Langevin, 156*X Centre de Tri,* 38042 *Grenoble, France*

(*Received* 5 *February* 1982; *accepted* 10 *May* 1982)

Abstract

The structure of O-excess perovskite $BaUO_{3+x}$ has been examined by powder neutron diffraction at room temperature. The non-stoichiometry is clearly shown to arise from an equivalent number of Ba and U vacancies in a compound of overall composition $BaUO_{3\cdot30(3)}$. As expected, the temperature factors are larger in the disordered compound than in a compound close to the stoichiometric ideal of $BaUO_3$ which has also been structurally refined. A previous report that $BaUO_3$ is at least partially oxidized at room temperature in oxygen is confirmed. [$BaUO_{3\cdot30}$: *Pnma*, $a = 6\cdot2094$ (13), $b = 8\cdot7987$ (19), $c = 6\cdot2370$ (15) Å, $R_p = 16\cdot0\%$, $R_w = 13\cdot9\%$, $R_{exp} = 13\cdot1\%$ for 252 overlapping reflections; $Ba_{0\cdot98}UO_3$: *Pnma*, $a = 6\cdot1999$ (31), $b = 8\cdot7644$ (64), $c = 6\cdot2075$ (35) Å, $R_p = 8\cdot7\%$, $R_w = 10\cdot1\%$, $R_{exp} = 4\cdot2\%$ for 540 overlapping reflections.

Introduction

Ternary uranium oxide systems, are, in general, complex. Most of the known phases have been prepared by reactions of the stoichiometric metal oxides (or carbonates *etc.*) with one of the stoichiometric uranium oxides, but there is often a question whether the reported 'phases' are always discrete stoichiometric compounds or whether they are frequently (particularly at high temperature) simply

0567-7408/82/112775-07$01.00

members of a broad non-stoichiometric phase. Very little is known about the non-stoichiometric properties of most of the mixed uranium oxides and this present study is directed towards one system of particular interest – $BaUO_{3+x}$ – which represents a relatively rare example of an O-excess perovskite.

Tofield & Scott (1974) have investigated oxidative non-stoichiometry in perovskite systems, examining the range of excess O for $LaMnO_{3+x}$, $LaVO_{3+x}$, $Sr(La^{3+})TiO_{3+x}$, $LaCrO_3$, $LaFeO_3$ and $EuTiO_3$. The latter three systems did not show any tendency to oxidize and negligible solubility of La^{3+} was observed in $SrTiO_3$. However, for $LaVO_{3+x}$ ($x \lesssim 0{\cdot}05$) and for $LaMnO_{3+x}$ ($x \lesssim 0{\cdot}20$) there was no observable secondary phase (*e.g.* La_2O_3) in the X-ray diffraction patterns. $LaMnO_{3{\cdot}12}$ was studied by neutron diffraction with a comparison of integrated intensity refinements for models involving equal *A*- and *B*-site vacancies, *A* vacancies alone, *A* vacancies and *A* cations on *B* sites to complete *B*-site stoichiometry, and unequal *A*- and *B*-site vacancies. The results were interpreted in terms of the latter model with the composition $(La_{0{\cdot}94\pm0{\cdot}02}\ \square_{0{\cdot}06\pm0{\cdot}02})(Mn^{3+}_{0{\cdot}745}\ Mn^{4+}_{0{\cdot}235}\ \square_{0{\cdot}02})O_3$. The overall O excess in $BaUO_{3+x}$ is, however, larger than in any of these systems, and even more remarkably it absorbs oxygen at room temperature. Trzebiatowski & Jablonski (1960) report a gradually decreasing lattice constant up to a maximum value of $x = 0{\cdot}36$, above which $BaUO_4$ appears. There is no marked change in the measured density of $BaUO_{3+x}$ with increasing x, so they ascribe the O excess to anion interstitials. However, Braun, Kemmler-Sack, Roller, Seemann & Wall (1975) have investigated the BaO–UO_2–O system in detail and claim that monophasic mixed oxides with Ba:U ratio of 1:1 do not exist but are intrinsically biphasic – a perovskite phase with a small amount of fluorite phase (possibly UO_2).

In the present work we describe attempts to prepare the pure $BaUO_{3+x}$ phase at different compositions and the complete structural characterization of $BaUO_3$ and $BaUO_{3{\cdot}3}$ by powder neutron diffraction.

Experimental

Preparation and characterization of $BaUO_{3+x}$ *compounds*

Several methods have been investigated:

(i) The hydrogen reduction of $BaUO_4$ at 1373 K was employed to give a compound of estimated composition $BaUO_{\sim3{\cdot}23}$ ($a = 4{\cdot}40$ Å) contaminated with a small amount of a secondary fluorite phase with a lattice parameter $a = 5{\cdot}47$ Å (sample *A*, see below). Both $BaUO_4$ and Ba_3UO_6 (see below) were prepared by reactions of $BaCO_3$ (Johnson-Matthey 'Specpure' reagent) with UO_3 (Cerac 99·99%) or uranyl nitrate hexahydrate in air at about 1377 K. The reactions were carried out over several days and the samples characterized by X-ray powder diffraction and IR spectroscopy.

(ii) The reaction of Ba_3UO_6 with UO_2 was carried out under hydrogen at temperatures between 1423–1473 K for 12–24 h. High temperatures were necessary to reduce the U^{VI} to U^{IV} but they obviously increase the risk of the loss of BaO. Stoichiometric mixtures yielded a very dark brown sintered product, the surface of which was much lighter brown with white specks. This effect was presumed to be due to surface volatilization of BaO and the surface layers could be easily removed by scraping. The bulk of the sample was characterized by X-ray diffractometer patterns which showed only a very small fluorite-phase content and the pseudocubic perovskite phase ($a_o = 4{\cdot}39_5$ Å). No BaO, BaO_2 or $BaCO_3$ reflections could be observed in the pattern. Weight-change measurements – if only oxygen loss had occurred – indicated reduction to $BaUO_{3{\cdot}04}$ but this estimate is very sensitive to the loss of BaO by evaporation. The possibility of BaO loss was compensated for by providing a 3% excess of Ba_3UO_6 to react with UO_2 under a hydrogen flow at 1453 K for 36 h. The product was dark brown, again with a light brown surface which was removed. The X-ray diffractometer pattern showed it to be a single pseudocubic phase with $a_o = 4{\cdot}39$ Å (Trzebiatowski & Jablonski, 1960). This sample (*B*) (8 g) was at all times handled in a dry inert atmosphere to prevent any possibility of oxidation.

Several known weights of sample *B* were heated to constant weight at 1373 K (attained in about 72 h). Unlike the observations of Braun *et al.* (1975) only $BaUO_x$ was observed by powder X-ray diffraction, indicating a Ba:U ratio close to unity. Atomic absorption and high-precision polarography techniques, however, indicated some Ba deficiency at 0·94 (2):1. From the difference in weights on firing, the O/U ratio was determined as 2·83 (20):1.

(iii) High-pressure preparations were attempted by the reaction of BaO (Specpure, refired under high vaccuum at 1073 K for 48 h) with the stoichiometric proportion of UO_2 (Koch-Light 99·9%, refired in hydrogen at 1323 K for 20 h). The mixture was packed in boron nitride capsules and heated at 1573 K with pressures between 2·5 and 4·5 GPa, using a high-pressure belt apparatus. This method ensures a sealed system and no possibility of BaO loss.

The resultant medium brown products were characterized by Debye–Scherrer X-ray photographs and displayed lines of a fluorite phase as well as those of the pseudocubic '$BaUO_3$' phase. There were also other weak impurity lines. A high-pressure preparation of $BaUO_{3+x}$ was also attempted using the reaction mixture of $Ba_3UO_{5{\cdot}66}$ + $2UO_2$. Under conditions similar to those described above a single phase could not be produced.

The reduction and reoxidation of $BaUO_{3+x}$

The reported ease of oxidation of $BaUO_3$ in air has been re-examined under controlled conditions. Part of the $BaUO_{3+x}$ sample (*A*) prepared as in (i) above was reduced in hydrogen at 1423 K for 20 h. The weight change indicated that reduction to $BaUO_3$ occurred although a BaO surface layer was again found. The sample was extracted in a dry inert atmosphere, the surface layers removed, and characterized by high-precision X-ray diffractometry (stepping in $0{\cdot}01°2\theta$) using a specially designed sample cell which enabled the compound to be kept in an atmosphere of dry hydrogen. The presence of a fluorite phase [a_o = 5·468 (8) Å] persisted in the product together with a pseudocubic phase [$a_o = 4{\cdot}400$ (1) Å]. This latter value should be compared with 4·402 (1) Å found by Trzebiatowski & Jablonski as the maximum in the system $BaUO_{3+x}$ and which has been claimed to be characteristic of $x = 0$.

A weighted amount of the sample (~1 g) contained in a gold boat was subjected to a flow of pure dried oxygen at 297 K for several days. The weight of the sample was found to increase steadily over the period as indicated in Fig. 1. After five days the sample [with composition $BaUO_{3{\cdot}051(4)}$] was re-examined by X-ray diffraction. There was no obvious change in the ratio of fluorite phase:perovskite phase intensities, nor could any new reflections be detected. The lattice parameters were calculated as: fluorite phase, a_o = 5·464 (3) Å; perovskite phase, $a_o = 4{\cdot}389$ (1) Å.

Our sample did not take up oxygen as rapidly as that of Trzebiatowski & Jablonski (1960) in air. This may be due to a larger particle size in our case or it could be associated with the reaction of free BaO with water or CO_2 in the earlier study.

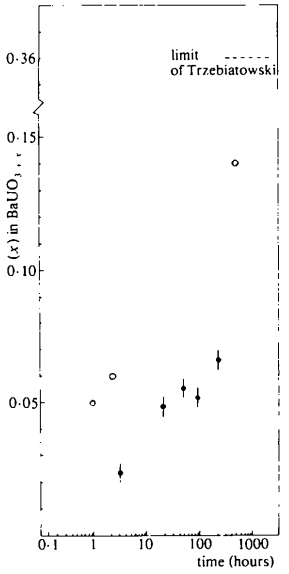

Fig. 1. Controlled oxidation of $BaUO_3$ sample. ♦ this work, O Trzebiatowski & Jablonski (1960). [The value of x assumes negligible UO_2 content – see text for validity of this assumption.]

The main part of the uptake of oxygen in the present experiment cannot be ascribed to the reaction $BaO \rightarrow BaO_2$ because neither BaO nor BaO_2 is detectable in the X-ray pattern. Assuming that the fluorite phase is UO_2 the absence of U_3O_8 reflections in the X-ray pattern of $BaUO_{3{\cdot}05}$ shows that a gross oxygen take-up by UO_2 is not important. The fluorite phase was estimated as <10% according to the X-ray analysis and its lattice parameter, identical to that of UO_2 within the estimated error, does not appear to change, indicating that oxygen uptake by this phase is negligible. For the pseudocubic perovskite phase there is, however, a distinct decrease in the lattice parameter similar in magnitude to that noted by Trzebiatowski & Jablonski (1960).

Neutron diffraction on sample A ($BaUO_{3{\cdot}3}$)

Powder neutron diffraction studies were carried out on the O-excess sample *A* on the PANDA diffractometer at AERE Harwell at a neutron wavelength of 1·5 Å. The sample was contained in a thin-walled vanadium can. Reflections characteristic of the $GdFeO_3$-type orthorhombic structure are observed in the neutron pattern, see Fig. 2.* Peaks of the fluorite phase are also evident (the strongest is indicated in the legend for Fig. 2) and we assume this to be UO_2 from the lattice parameter.

Possible structural models

Given the presence of $BaUO_{3+x}$, either alone or with UO_2, five structural schemes can be envisaged to

* The numerical data corresponding to Figs. 2 and 3 have been deposited with the British Library Lending Division as Supplementary Publication No. SUP 36953 (6 pp.). Copies may be obtained through The Executive Secretary, International Union of Crystallography, 5 Abbey Square, Chester CH1 2HU, England.

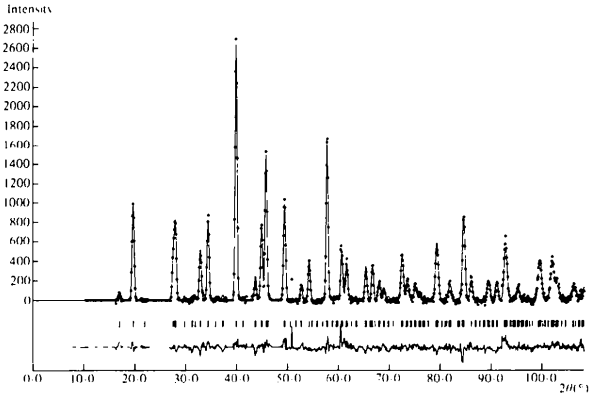

Fig. 2. Neutron powder diffraction pattern of $BaUO_{3{\cdot}3}$. Reflections of the $GdFeO_3$ orthorhombic structure and UO_2 are shown together with the difference profile (lower curve). The 5th and 8th reflections are respectively the 111 and 200 reflections of UO_2.

account for the composition $BaUO_{3+x}$ as shown in Table 1. No perovskite system is known with substantial random O interstitials as in scheme 1 although incorporation of additional O, as for example in $La_2Ti_2O_7$–$CaTiO_3$, can occur by periodic crystallographic shear (Nanot, Queyroux & Gilles, 1977). The situation in scheme 2 is similar to that responsible for oxidative non-stoichiometry in $LaMnO_{3+x}$. Scheme 3 involves only *B*-cation vacancies and no system is known with such random vacancies. (However, interleaving of perovskite layers with A_2O_2 layers or with h.c.p. stackings can produce this effect.) Scheme 4 is an *A*-cation variant of the perovskite scheme $Ba_{3-x}U_{1+x}O_6$ (having Ba_3UO_6 as the limiting composition) investigated by Braun *et al.* (1975). Scheme 5 is the result of BaO being taken into solid solution in $BaUO_3$ which apparently occurs with an increase in the pseudocubic lattice parameter up to a maximum composition Ba_3UO_5 (Trzebiatowski & Jablonski, 1960). Above the composition $0{\cdot}5BaO{:}BaUO_3$ this phase displays the X-ray superstructure reflections of the $(NH_4)_3FeF_6$ cryolite-type structure.

Oxygen interstitials in the perovskite structure could only be accommodated in the (A_2B_4) octahedral sites or in the smaller tetrahedral sites of the AO_3 cubic-close-packed lattice. The equivalent sites in the *Pnma* structure of $BaUO_{3+x}$ with 4Ba at $(\sim 0, \frac{1}{4}, \sim 0)$ and 4U at $(\frac{1}{2}, 0, 0)$ are 4 at (0, 0, 0), 4 at $(\sim\frac{1}{4}, \frac{1}{4}, \sim\frac{1}{4})$ and 4 at $(\sim\frac{1}{4}, \frac{1}{4}, \sim\frac{3}{4})$ for the octahedral interstices and 32 at $(\sim\frac{1}{4}, \sim\frac{1}{8}, \sim 0$, *etc.*) for the tetrahedral interstices.

Neutron refinements

The diffraction pattern was analysed by the method of profile analysis (Rietveld, 1967, 1969). The Rietveld method minimizes the function

$$\chi^2 = \sum_i w_i |y_i(\text{obs}) - (1/c) y_i(\text{calc})|^2$$

where $y_i(\text{obs})$, $y_i(\text{calc})$, $w_i = [1/y_i(\text{obs})]$ and c are the observed intensity at the position 2θ, the calculated intensity, the assigned weight and the scale factor respectively. The program calculates a weighted profile *R* factor:

$$R_{wp} = 100\left\{\sum_i w_i[y_i(\text{obs}) - (1/c)y_i(\text{calc})]^2 / \times \sum_i w_i[y_i(\text{obs})]^2\right\}^{1/2}$$

and there is also an expected *R* factor:

$$R_E = 100\left\{(N - P + C)/\sum_i w_i[y_i(\text{obs})]^2\right\}^{1/2}$$

which we might expect to obtain if the differences between the observed and calculated profiles are purely statistical in origin. The quantity $N - P + C$ is the number of degrees of freedom where N is the number of statistically independent observations, P is the number of least-squares parameters and C the number of constraint functions. The scattering lengths used were Ba = 5·25, U = 8·53 and O = 5·8 fm.

Regions of the diffraction pattern containing the fluorite phase were excluded from a Rietveld profile refinement. The five schemes discussed above were accommodated (i) by introducing octahedral or tetrahedral O interstitials (scheme 1), and (ii) by refining the apparent occupation numbers of Ba and U sites individually or separately (schemes 2 to 5). The stoichiometric model $BaUO_3$ and the *A*-site vacancy model $Ba_{1-x}UO_3$ were also refined for the sake of comparison.

Refinements of type (i) indicated negligible occupancy levels of the interstitial positions. Fourier difference maps supported this as no difference peaks were observable in either the expected octahedral or tetrahedral interstices. None of the refinements suggested either excess of Ba or a Ba-only deficiency. The best fit was obtained using the scheme in which both Ba and U occupations were each varied and this gave an R_{wp} of 17·6% (expected 11·5%) on the basis of $Ba_{0\cdot96\,(2)}U_{0\cdot93\,(2)}O_3$.

Bendall & Thomas (1978) have recently revised the Rietveld program to allow the simultaneous refinement of up to three phases and this has been used in a refinement of the complete data. The initial parameters for $BaUO_{3+x}$ were derived from the fit derived above

Table 1. *Possible structural models giving a perovskite phase of composition* $BaUO_{3+x}$

Scheme	ABO_3 formula	Secondary phase	Value of y	U^{IV}/U^{V} formulation	U^{IV}/U^{VI} formulation	Description
1	$BaUO_{3+x}$	—	—	$Ba\,(U^{IV}_{1-2x}U^{V}_{2x})O_{3+x}$	$Ba(U^{IV}_{1-x}U^{VI}_{x})O_{3+x}$	Oxygen interstitials
2	$Ba_{1-y}U_{1-y}O_3$	—	$y = x/3 + x$	$Ba_{1-y}(U^{IV}_{1-7y}U^{V}_{6y})O_3$	$Ba_{1-y}(U^{IV}_{1-4y}U^{VI}_{5y})O_3$	Equivalent numbers of *A*- and *B*-site vacancies
3	$Ba_{1-y}(U_{1-y}Ba_y)O_3$	$+yUO_2$	$y = x/2$	$Ba_{1-y}(U^{IV}_{1-5y}U^{V}_{4y}Ba_y)O_3$	$Ba_{1-y}(U^{IV}_{1-3y}U^{VI}_{2y}Ba_y)O_3$	*A*-site vacancies produced by *A* cations on *B* sites
4	$Ba(U^{IV}_{1-y}Ba_y)O_3$	$+yUO_2$	$y = x$	—	—	*A* cations substituting for *B* cations
5	$BaU_{1-y}O_3$	$+yUO_2$	$y = x/2$	$Ba(U^{IV}_{1-5y}U^{V}_{4y})O_3$	$Ba(U^{IV}_{1-3y}U^{VI}_{2y})O_3$	*B*-site vacancies

and the secondary fluorite phase was assumed to be uranium dioxide and refined as UO_{2+y}. The refinements on this basis converged rapidly to give R_{wp} = 14·7% (expected 13·2%) with the second phase refining as $UO_{2\cdot05\pm0\cdot71}$. The uncertainty in the occupation number of O in UO_2 is very large, not only because only a relatively small amount was present but also because there are few fluorite reflections and those with $h + k + l = 4n + 2$ are of low intensity. However, models incorporating initially either a large O excess or deficiency in the $UO_{2\pm x}$ phase always refined close to $UO_{2\cdot0}$. Characterization of the secondary phase as UO_2 was supported by the refined lattice constant [5·456 (5) Å] which is, within estimated errors, identical to that of the UO_2. That no O excess was observed in the UO_2 is reasonable in view of the reducing conditions utilized in the preparation.

The complete pattern was finally refined allowing the occupancies Ba and U to vary as $Ba_{1-x}U_{1-y}O_3$ together with UO_2. An R_w factor of 13·9% (expected 13·1%) was obtained, corresponding to $Ba_{0\cdot911(11)}U_{0\cdot909(9)}O_3$. The Ba and U occupancies thus appear to be equal and the composition is $BaUO_{3\cdot30(3)}$. The refinement details are summarized in Table 2 with the derived bond lengths and angles in Table 3. The profile fit is illustrated in Fig. 2.

Neutron diffraction on sample B ($Ba_{0\cdot98}UO_3$)

The neutron diffraction pattern for sample *B* was measured on the D2 diffractometer at the Institut Laue–Langevin, Grenoble, using a wavelength of about 1·22 Å.

The diffraction profile recorded at 295 K was refined by the Rietveld procedures using similar models to those employed for the analysis of $BaUO_{3\cdot3}$. No fluorite reflections could be detected in the pattern, which implied a UO_2 content in the samples less than about 2%. It was necessary only to exclude a small region (1·5°) of the 2θ scan where an aluminium peak interfered with the pattern.

The models refined were (i) $BaUO_3$ (the stoichiometric composition), (ii) $Ba_{1-y}UO_3$ [which gave a Ba content of 0·98 (1)], and (iii) $Ba_{1-y}UO_{3-x}$ (O content variable; Ba:U ratio fixed from the chemical analysis given above, which refined to $Ba_{0\cdot94}UO_{2\cdot99}$). The R_{wp} factors are very similar for each of these three refinements: 10·2, 10·1 and 10·2 respectively. Given that the chemical analysis indicates a Ba deficiency which is probably too high (no UO_2 was detected in the

Table 2. *Refined parameters for* $BaUO_{3\cdot30}$ + UO_2 *(secondary phase) (298 K); simultaneous profile refinement of both phases*

(I) $BaUO_{3\cdot30}$, orthorhombic, space group *Pnma*

	Position	*x*	*y*	*z*	*B* (Å²)	Occupation number, *N*
Ba	4(*c*)	0·0042 (47)	0·25	−0·0053 (41)	2·03 (18)	0·911 (1)
U	4(*b*)	0·5	0	0	0·74 (7)	0·909 (1)
O(1)	4(*c*)	0·5007 (6)	0·25	0·0512 (26)	2·89 (10)	1·0
O(2)	8(*d*)	0·2694 (3)	0·0400 (11)	−0·2618 (22)	2·89 (10)	2·0

(II) UO_2, cubic, space group $Fm3m$, a_o = 5·4682 (21) Å

	x	*y*	*z*	*B* (Å²)
U	0	0	0	0·38 (85)
O	0·25	0·25	0·25	0·58 (97)

R_p = 16·0%, R_w = 13·9%, R_{exp} = 13·1%

Table 3. *Derived bond distances* (Å) *and angles* (°) *for* $BaUO_{3\cdot30}$

U–O(1)	2·223 (2)	O(1)–U–O(1)	180·0
U–O(2)	2·199 (16), 2·265 (17)	O(2)–U–O(2)	180·0
			88·2 (6), 91·8 (6)
Ba–O(1)	3·103 (49), 2·832 (21)	O(1)–U–O(2)	87·1 (8)
	3·405 (31), 3·146 (49)		92·9 (8)
Ba–O(2)	2·947 (26)		86·5 (8)
	2·766 (25)		93·5 (8)
	3·285 (21)		
	3·489 (23)		

Table 4. *Refined parameters for* $Ba_{0\cdot98}UO_3$ *at* 295 K *(profile refinement, orthorhombic symmetry, space group Pnma)*

	Position	*x*	*y*	*z*	*B* (Å²)	Occupation number, *N*
Ba	4(*c*)	0·0240 (15)	0·25	0·0060 (26)	0·16 (9)	0·976 (8)
U	4(*b*)	0·5	0	0	0·35 (5)	1·001 (7)
O(1)	4(*c*)	−0·0235 (17)	0·25	0·5761 (15)	1·03 (5)	1·0
O(2)	8(*d*)	0·7700 (14)	0·0288 (6)	0·2351 (15)	1·03 (5)	2·0

R_p = 8·7%, R_w = 10·1%, R_{exp} = 4·2%

Table 5. *Interatomic distances* (Å) *and angles* (°)

U–O(1)	2·246 (3)	O(1)–U–O(1)	180·0
U–O(2)	2·191 (9), 2·235 (9)	O(2)–U–O(2)	180·0
			90·8 (3), 89·2 (3)
Ba–O(1)	2·682 (18), 3·436 (14)	O(1)–U–O(2)	85·7 (3)
	2·855 (14), 3·546 (18)		94·3 (3)
			89·8 (3)
Ba–O(2)	2·874 (12)		90·2 (3)
	2·944 (12)		
	3·137 (11)		
	3·436 (14)		

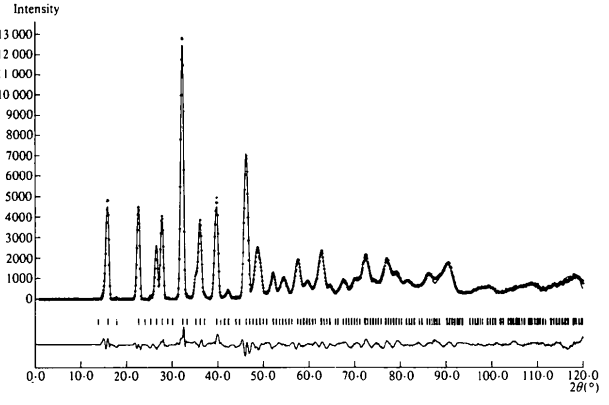

Fig. 3. Neutron powder diffraction pattern of $Ba_{0\cdot98}UO_3$. Orthorhombic reflections are shown, and the difference profile (lower curve).

diffraction patterns), we prefer the refinement which gives $Ba_{0.98}UO_3$. Fourier difference maps based on this refinement showed no extra features and although the R_{wp} is considerably larger than R_E (4·2%) the fit is satisfactory for the D2 diffractometer which has a relatively high background.

The parameters and derived bond lengths and angles for $Ba_{0.98}UO_3$ are shown in Tables 4 and 5 respectively and the profile fit is illustrated in Fig. 3.*

Discussion

It can be seen that in $Ba_{0.98}UO_3$ the temperature factors for all the atoms, especially Ba, are lower than in $BaUO_{3.3}$. In fact they are representative of a typical stoichiometric perovskite and the O temperature factors in particular are similar to those found for KUO_3 and $NaUO_3$ at similar temperatures (Barrett & Fender, 1982). This suggests, in agreement with a composition of $Ba_{0.98}UO_3$, that only one type of UO_6 octahedron is present in the structure.

The larger effective ionic radius of six-coordinate U^{4+} (0·98 Å, Shannon & Prewitt, 1969) than of, say, Ti^{4+} (0·605 Å) makes it likely that the unit-cell parameter of barium uranate perovskites is determined by U—O repulsions rather than by Ba—O interactions. This view is supported by the pseudocubic lattice constants of $BaUO_{3+x}$ (4·40 Å) which are considerably larger than for $BaTiO_3$ (4·00 Å) and by the longer than normal Ba—O separations (3·12 Å); compare 2·84 Å for $BaTiO_3$ and 2·96 or 3·01 Å for the sum of the effective ionic radii of Ba^{2+} and O^{2-} (1·35 or 1·40 Å). We have previously (Jacobson, Tofield & Fender, 1972) reviewed effective ionic radii in perovskites and demonstrated that the two-coordinate radius of O^{2-} (1·35 Å) is appropriate to materials such as $BaUO_3$. The average U—O separation in $Ba_{0.98}UO_3$ is 2·224 Å yielding an effective radius of 0·874 Å for U^{4+} in very acceptable accord with a value of almost 0·88 Å quoted by Knop & Carlow (1974).

$BaUO_{3.3}$ provides the clearest example of a non-stoichiometric perovskite with *B*-site vacancies. Compared with $LaMnO_{3.12}$ (where it is in fact difficult to prove conclusively the presence of the 2% Mn vacancy concentration) the vacancy concentration, 9%, is large. Other examples of *B*-cation-vacancy perovskites, several of which contain U^{6+}, have been reported by Rauser & Kemmler-Sack (1980). *B*-site vacancy concentrations ranging between 0·06 and 0·17 have been observed although no structural details have been reported.

In the study of $LaMnO_{3+x}$ it was observed that the large decrease in effective ionic radius from Mn^{3+} to Mn^{4+} (18%) might assist the stabilization of *B*-site vacancies. A similar situation pertains to U where the effective ionic radii of octahedral U^{5+} (0·76 Å; Shannon & Prewitt, 1969) and U^{6+} (0·73 Å; Shannon & Prewitt, 1970) are 13 and 16% respectively lower than that of octahedral U^{4+} as determined above.

In contrast to $LaMnO_{3+x}$, oxidation of $BaUO_4$ does not bring about a significant reduction in the average U—O distance and the volume of the unit cell contracts to only a small extent. The explanation is almost certainly implicit in the abnormally high O temperature factor [2·9 (1) Å^2] which indicates a reduction in certain U—O distances, presumably arising from relaxation towards the cation of O atoms which lie between a U cation and a U vacancy. In this respect $BaUO_{3+x}$ appears to be analogous to α-UO_3 (Greaves & Fender, 1972) in which U vacancies are stabilized by the formation of shorter U—O bonds.

The O temperature factor implies a static displacement of about 0·1 Å. Quite large static displacements are to be expected because, if we consider the U environment alone, six different types of O bridges can be envisaged, *viz* U^{IV}—U^{IV}; $U^{V/VI}$—U^{IV}; $U^{V/VI}$—$U^{V/VI}$; U^{IV}—U(vacancy); $U^{V/VI}$—U(vacancy); U(vacancy)—U(vacancy), which will give rise to a range of O positions about the determined mean. Because of the large number of different O positions the overall diffuse scattering is not significantly modulated, but is simply distributed into a rising (with 2θ) background in a manner indistinguishable from thermal diffuse scattering. We note also that the large temperature factors for Ba and U also show the effect of the disordered structure, with the effects, as expected, greater for the Ba atoms which are incorporated in the O layers.

We are grateful to the Science and Engineering Research Council and AERE Harwell for providing neutron diffraction facilities, and to the University Support Group at Harwell for experimental assistance. One of us (SAB) thanks AERE Harwell for financial support during a period of postgraduate study.

* See deposition footnote.

References

BARRETT, S. A. & FENDER, B. E. F. (1982). To be published.

BENDALL, P. J. & THOMAS, M. W. (1978). *Acta Cryst.* A**34**, S351.

BRAUN, R., KEMMLER-SACK, S., ROLLER, H., SEEMANN, I. & WALL, I. (1975). *Z. Anorg. Allg. Chem.* **415**, 133–155.

GREAVES, C. & FENDER, B. E. F. (1972). *Acta Cryst.* B**28**, 3609–3614.

JACOBSON, A. J., TOFIELD, B. C. & FENDER, B. E. F. (1972). *Acta Cryst.* B**28**, 956–961.

KNOP, O. & CARLOW, J. S. (1974). *Can. J. Chem.* **52**, 2175–2183.

NANOT, M., QUEYROUX, F. & GILLES, J.-C. (1977). *J. Phys.(Paris)*, **38**(C7), 91–94.

RAUSER, G. & KEMMLER-SACK, S. (1980). *J. Solid State Chem.* **33**, 135–140.
RIETVELD, H. M. (1967). *Acta Cryst.* **22**, 151–152.
RIETVELD, H. M. (1969). *J. Appl. Cryst.* **2**, 65–71.
SHANNON, R. D. & PREWITT, C. T. (1969). *Acta Cryst.* B**25**, 925–946.
SHANNON, R. D. & PREWITT, C. T. (1970). *Acta Cryst.* B**26**, 1046–1047.
TOFIELD, B. C. & SCOTT, W. R. (1974). *J. Solid State Chem.* **10**, 183–194.
TRZEBIATOWSKI, W. & JABLONSKI, A. (1960). *Nukleonika*, **5**, 587–596.

Acta Cryst. (1982). B**38**, 2781–2784

Pentadecacopper(II) Bisdiborate Hexaorthoborate Dioxide

BY HELMUT BEHM

Institut für Kristallographie der Universität Karlsruhe (TH), D-7500 Karlsruhe, Federal Republic of Germany

(*Received* 6 *December* 1981; *accepted* 19 *May* 1982)

Abstract

$Cu_{15}[(B_2O_5)_2|(BO_3)_6|O_2]$ with the oxide formula $3CuO.B_2O_3$ crystallizes in space group $P\bar{1}$ with a = 3·353 (2), b = 19·665 (7), c = 19·627 (8) Å, α = 88·77 (3), β = 69·71 (2), γ = 69·24 (2)°, Z = 10, D_x = 4·51, D_m = 4·4 Mg m^{-3}, μ(Mo $K\alpha$) = 13·95 mm^{-1}; R = 0·03 for 3407 reflections contributing to the refinements. $3CuO.B_2O_3$ builds up a layer structure. The structure consists of almost planar B_2O_5 groups, planar isolated BO_3 groups, isolated O^{2-} ions, and Cu^{2+} ions with a fourfold planar coordination. It is the first reported structure with isolated B_2O_5 and BO_3 groups in conjunction with isolated O^{2-} ions.

Introduction

In the binary system CuO–B_2O_3 only two compounds have been reported by Weir & Schroeder (1964), Ecker (1966), Lecuir & Guillermet (1971), Martínez-Ripoll, Martínez-Carrera & García-Blanco (1971), Uhlig (1976), and Richter (1976). These compounds have molar ratios of copper oxide to boron oxide of 1:1 and 3:1. The structure of the metaborate $CuO.B_2O_3$ has been determined by Martínez-Ripoll *et al.* (1971). Until now only infrared and X-ray powder data of $3CuO.B_2O_3$ were available. Infrared spectra show, however, that the structure of $3CuO.B_2O_3$ must be more complex than that of other compounds with formula $3MO.B_2O_3$ (M = Mg, Mn, Co, Ni) which have been studied in detail.

Experimental

Single crystals of $3CuO.B_2O_3$ were grown in a platinum crucible from a nearly stoichiometric melt (3% excess B_2O_3). Most crystals obtained by this method were in the form of thin plates, frequently intergrown. They all showed perfect cleavage on (100) and the form {100} was the most prominent. For the X-ray investigations a nearly isometric crystal with natural forms {100}, {011}, {0$\bar{1}$1}, and {001} was selected. The dimensions of the pinacoidal crystal could be described by the distances of the faces from crystal centre with: (100) 32, (011) 18, (0$\bar{1}$1) 31, and (001) 22 μm.

The space group and crystal data were determined by equi-inclination Weissenberg and precession photographs, using Cu $K\alpha$ radiation. Lattice constants were refined from 16 Bragg reflections, measured on a Picker diffractometer. The lattice parameters were reduced using Delaunay's method. The unreduced cell (the setting of which is closely related to the crystal shape) proved to be more convenient in the following considerations.

Data collection: 8500 reflections, 3·5° ≤ 2θ ≤ 50°, Picker four-circle diffractometer, graphite monochromator, Mo $K\alpha$ radiation, $\theta/2\theta$ scan, scan speed 0·5° min^{-1}, scan range $\Delta 2\theta$ = 2° plus dispersion correction, background 2 × 40 s, three standard reflections every 50 reflections with variations ≤3%. Data reduction: XRAY system (1976) on a Univac 1108 computer, Lorentz and polarization corrections (XRAY system, *DATCO5*, *DATRDN*), absorption correction, using the Gaussian quadrature method (XRAY system, *ABSORB*) with 7 × 7 × 7 sample points and the optically measured crystal dimensions as listed above. After averaging 3939 symmetrically independent reflections, 2724 had $I(hkl) > 5\sigma(I)$; $\sigma(I)$ from counting statistics.

Structure determination

Since direct methods failed, Patterson maps were used. They showed the presence of a nearly planar tetragonal layer structure, with the layers having almost tetragonal symmetry. Polarized infrared single-crystal measurements also indicated that B should be coordinated in a planar fashion to three O atoms and that all

0567-7408/82/112781-04$01.00